View metadata, citation and similar papers at core.ac.uk

brought to you by CORE

provided by Ghent University Academic Bibliography

Solid-state formation of titanium carbide and molybdenum carbide as contacts for carbon-containing semiconductors

W. P. Leroy,[a] C. Detavernier,[b] and R. L. Van Meirhaeghe
Vakgroep Vaste-Stofwetenschappen, Ghent University, Krijgslaan 281/S1, B-9000 Gent, Belgium

A. J. Kellock
IBM Research Division, Almaden Research Center, San Jose, California 95120

C. Lavoie[c]
IBM T.J. Watson Research Center, Yorktown Heights, New York 10598 and Engineering Physics Department, Ecole Polytechnique de Montréal, Montréal, Quebec H3C 3A7, Canada

(Received 3 August 2005; accepted 6 February 2006; published online 20 March 2006)

Metal carbides are good candidates to contact carbon-based semiconductors (SiC, diamond, and carbon nanotubes). Here, we report on an *in situ* study of carbide formation during the solid-state reaction between thin Ti or Mo films and C substrates. Titanium carbide (TiC) was previously reported as a contact material to diamond and carbon nanotubes. However, the present study shows two disadvantages for the solid-state reaction of Ti and C. First, because Ti reacts readily with oxygen, a capping layer should be included to enable carbide formation. Second, the TiC phase can exist over a wide range of composition (about 10%, i.e., from $Ti_{0.5}C_{0.5}$ to $Ti_{0.6}C_{0.4}$), leading to significant variations in the properties of the material formed. The study of the Mo–C system suggests that molybdenum carbide (Mo_2C) is a promising alternative, since the phase shows a lower resistivity (about 45% lower than for TiC), the carbide forms below 900 °C, and its formation is less sensitive to oxidation as compared with the Ti–C system. The measured resistivity for Mo_2C is $\rho=59\ \mu\Omega\,\text{cm}$, and from kinetic studies an activation energy for Mo_2C formation of $E_a=3.15\pm0.15$ eV was obtained. © *2006 American Institute of Physics*. [DOI: 10.1063/1.2180436]

I. INTRODUCTION

Several carbon-based semiconductors are promising materials for future electronic applications. SiC offers significant advantages for high-power-switching devices.[1] Doped diamond is a superior wide-band-gap semiconductor, offering a high breakdown voltage, high thermal conductivity, small dielectric constant, and excellent radiation hardness.[2] Carbon nanotubes (CNTs) are quasi-one-dimensional molecular structures with semiconducting or metallic properties, which are widely investigated for application in the field of nanoelectronics.[3] While these advantages are being widely investigated, there is also a need for reliable contacts to these carbon-containing semiconductors.

In silicon-based technology, metal-silicon compounds (silicides) are now widely used as contact materials, since they offer several advantages as compared with metal contacts. Unlike pure metals, several silicide phases are thermodynamically stable in contact with silicon and, when silicides are formed by a solid-state reaction between metal and Si, contact formation can be achieved by means of a self-aligned process (SALICIDE).[4] The solid-state reaction between metal and Si only occurs in those regions of a patterned substrate where the metal is in direct contact with the Si (or C for the present case of carbides). Therefore, there is no need for alignment and lithographic patterning of the metal film, since the formation of the silicide will be automatically restricted to the contact region. One can expect the same advantages when using carbides to contact carbon-based semiconductors. While titanium has already been used to contact diamond[5,6] and CNTs,[7] relatively little work has been reported concerning carbide formation during thin film reactions.

In this work, we studied the formation of titanium carbide and molybdenum carbide through a solid-state reaction. Ti was chosen because of the existence of prior work.[5] While the Mo is shown to react with C at higher temperatures, the inactivity of Mo with respect to oxidation presents clear process advantages.

II. EXPERIMENT

The samples used in this work consisted of 30 nm Ti or Mo on different substrates: SiO_2, CNTs deposited on SiO_2, or 200 nm amorphous C on SiO_2. Sometimes capping layers were included (5 or 30 nm, amorphous C or TiN), and they will be mentioned where used. All layers were sputter deposited at a base pressure of 10^{-6} mbar. The sputtering equipment was calibrated prior to sample preparation, using several depositions of each metal and a Talystep profilometer.

Several techniques were used for this study: four point probe for resistance measurements, x-ray photoelectron spectroscopy (XPS) for phase composition information, Rutherford backscattering spectrometry (RBS) for contamination and thickness measurements, and *in situ* x-ray diffraction (XRD) for phase identification and for determining the acti-

[a]Electronic mail: wouter.leroy@ugent.be
[b]Electronic mail: christophe.detavernier@ugent.be
[c]Electronic mail: clavoie@us.ibm.com

 © 2006 American Institute of Physics

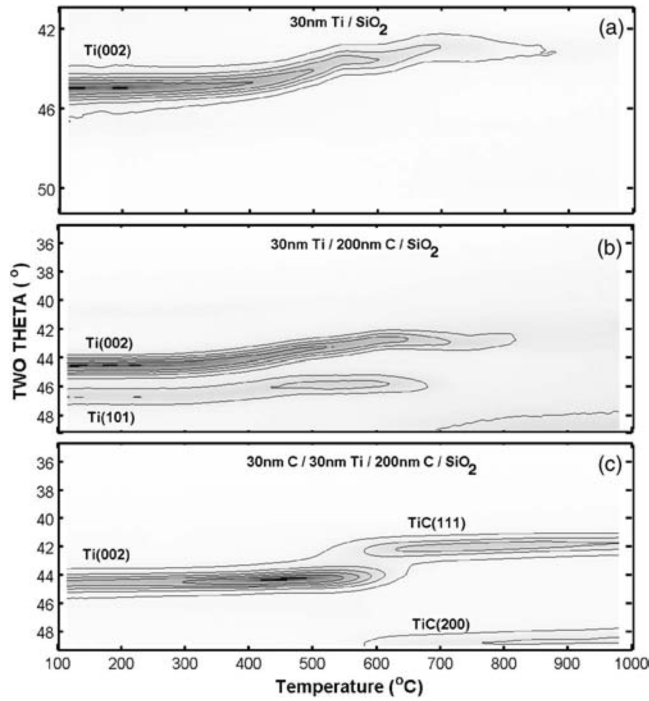

FIG. 1. *In situ* XRD pattern of 30 nm Ti deposited on (a) SiO_2, (b) 200 nm amorphous carbon on SiO_2, and (c) 200 nm amorphous carbon on SiO_2 with 30 nm carbon capping layer.

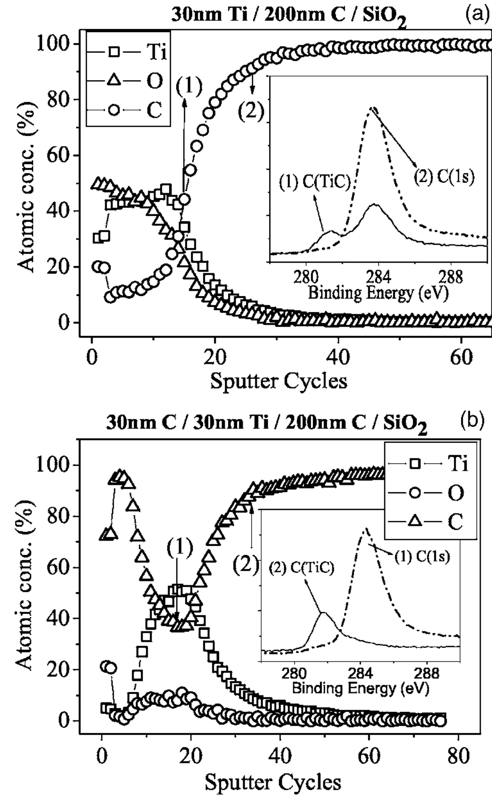

FIG. 2. XPS depth profiles of the Ti–C system (a) without a capping layer and (b) with a 30 nm C capping layer. Both samples were annealed to 1000 °C at 3 °C/s in a He atmosphere. The insets show the single C peak measured at the respective depths, marked with (1) and (2).

vation energy E_a. The *in situ* XRD experiments were performed at the X20C beam line of the National Synchrotron Light Source (NSLS) at Brookhaven National Laboratory. During annealing, the sample is continuously illuminated by an intense beam of monochromatic x rays ($\lambda=0.177$ to 0.180 nm). During the measurement, the samples were heated from 100 to 1000 °C in a purified He atmosphere, at different ramp rates (from 0.3 to 35 °C/s). Diffracted photons from the sample are continuously detected by an array of photodiodes covering 14° in 2θ. Acquisition times can vary from 100 ms to several minutes depending on the annealing conditions. For the standard heating rate of 3 °C/s presented here, a spectrum is taken every 0.5 s.

III. RESULTS AND DISCUSSION

A. The Ti–C system

Figure 1 shows *in situ* XRD patterns of 30 nm Ti deposited on SiO_2 and on 200 nm amorphous carbon (with and without a 30 nm carbon capping layer). The XRD data are presented both as contours and as a gray scale (black is the highest intensity). For the as-deposited sample, one can easily identify the Ti(002) peak near $2\theta\approx 45°$. Upon annealing to 1000 °C, this peak shifts towards lower 2θ values for samples without a C capping layer, indicating an expansion of the Ti lattice. This is caused by oxidation of the Ti layer, as confirmed by *ex situ* RBS analysis of quenched samples. This oxidation can either be a reaction with the oxygen impurities left in the annealing chamber or with oxygen from the substrate. An XPS measurement shown in Fig. 2(a) confirms that the uncapped Ti mainly oxidizes. However, analysis of the single C peak spectra showed that there is some TiC formation (insets in Fig. 2). The C spectrum at depth (1) shows a peak at lower binding energy (marked with "C(TiC)-peak") that indicates that there is TiC formation. The second spectrum in the insets show the standard C1*s* peak, and was obtained at depth (2), where no metal and thus no carbide formation are present.

When an extra 30 nm C layer is included as a capping layer, oxidation is prevented, and one observes the formation of a titanium carbide between $T_f^{\mathrm{TiC}}=550$ and 650 °C [Fig. 1(c)]. There are diffraction peaks around $2\theta\approx 42°$ and $\approx 49°$, corresponding to the (111) peak and the (200) peak of TiC. No other diffraction peaks could be observed from $2\theta \approx 35°$ to $\approx 70°$. Because there are also other possible phases of titanium carbide with diffraction peaks at these angles of 2θ (e.g., Ti_8C_5), XPS was performed on this sample. The formation of the TiC phase could be confirmed on the basis of the Ti/C ratio in the layer [Fig. 2(b)]. The difference in oxygen concentration between the samples with and without a capping layer is very clear.

From the above, it is clear that the sensitivity of Ti towards oxidation is a major problem when attempting to form TiC. A second problem of TiC is related to the solubility of C. TiC can be stable in a range of about 10% of C solubility.[8] With a lower C solubility, there will be C vacancies, which will act as powerful scattering centers for electrons and phonons. This will reflect itself in certain physical properties of the material, e.g., diffusion, thermal conductivity, and (most important) resistivity.[9,10] For instance, for the TiC layer formed in Fig. 1(c), a resistivity of $\rho=136\ \mu\Omega$ cm was measured using a standard four-point probe. Earlier work

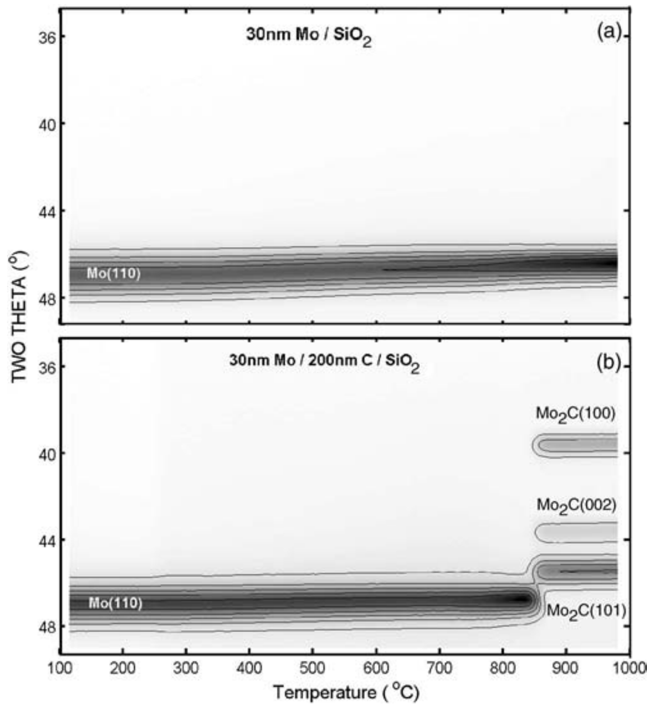

FIG. 3. *In situ* XRD patterns of 30 nm Mo deposited on (a) SiO_2 and (b) 200 nm C on SiO_2 without a capping layer (b). Samples were annealed to 1000 °C at 3 °C/s.

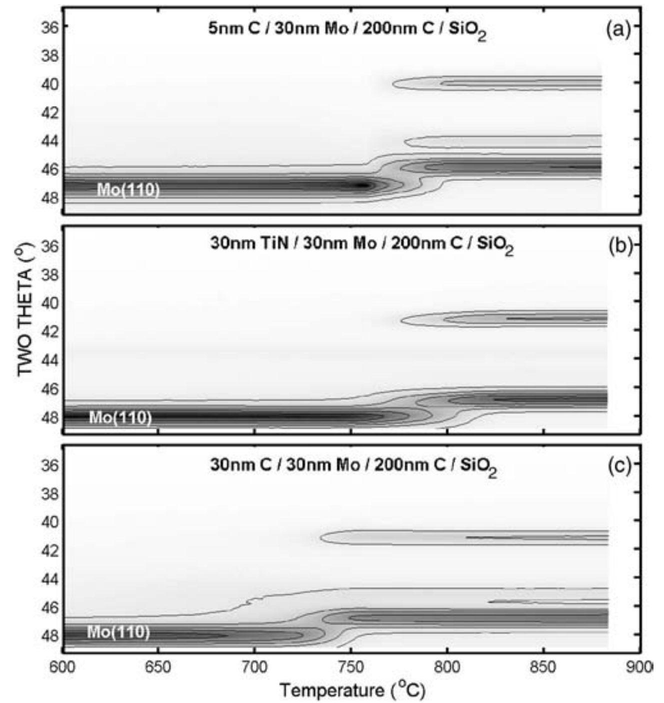

FIG. 4. *In situ* XRD patterns of 30 nm Mo deposited on 200 nm C on SiO_2 with (a) 5 nm C capping layer, (b) 30 nm TiN capping layer, and (c) 30 nm C capping layer. The samples were annealed to 1000 °C at 3 °C/s.

reports on values ranging from 35 to 250 $\mu\Omega$ cm. Williams[11] measured room-temperature resistivities for different C-vacancy concentrations (from $TiC_{0.93}$ to $TiC_{0.83}$). For stoichiometric TiC, Williams obtained a room-temperature resistivity of 70±10 $\mu\Omega$ cm. Up to 7% C vacancies, the resistivity shows a monotonic increase with increasing vacancy concentration, with an added resistivity of 16 $\mu\Omega$ cm per at. % of carbon vacancies in TiC. At higher vacancy concentrations (which means a lower C content, i.e., TiC_x with $x \leqslant 0.92$), the resistivity saturates around 200 $\mu\Omega$ cm. According to this model, our TiC films should have a C-vacancy concentration of about 4%. This is probably an upper limit, because impurities (such as oxygen) will also have an influence on the resistivity of the film.

A thickness for the TiC film was calculated from crystallographic data,[12] t=34.3 nm, which is in agreement with the RBS measurements (t=36.7±2 nm).

B. The Mo–C system

According to metal-C binary phase diagrams,[8] there are 14 metals other than Ti that can form stable carbide phases: Al, Sc, V, Cr, Mn, Fe, Y, Zr, Nb, Mo, Hf, Ta, W, and U. When we take a closer look at the binary phase diagrams, we see that only seven of these metal-C systems have a narrow range of composition (observed as a single vertical line on the binary phase diagrams): Al, Cr, Mn, Fe, Mo, W, and U, while the others exhibit carbide phases with a wide range of C solubility (such as Ti). From the compounds with a narrow range of composition, we have selected molybdenum as a good candidate, because of its relative insensitivity to oxygen. This is demonstrated in Fig. 3(a), where a 30 nm Mo layer on SiO_2 is annealed at 3 °C/s to 1000 °C, and no reaction is observed between the metal layer and the substrate, nor between the metal layer and the annealing atmosphere. In Fig. 3(b) the formation of Mo_2C can be seen between T_f =830 and 900 °C. As evidenced by the disappearance of the Mo(110) peak around $2\theta \approx 47°$, there is a clear phase transition from the metal phase to the Mo_2C phase. We can see carbide peaks around $2\theta \approx 40°$, $\approx 44°$, and $\approx 46°$, corresponding to the $Mo_2C(100)$, $Mo_2C(002)$, and $Mo_2C(101)$ planes, respectively. Other Mo_2C diffraction peaks could be observed when positioning the detector in other 2θ windows (not shown here). Figure 4 shows the solid-state reaction for a Mo sample with different capping layers: 5 and 30 nm C, and 30 nm TiN. The transition to Mo_2C was observed for all samples, although the formation temperature varied significantly: transition temperatures between $T_f^{5\text{ nm C}}$=730 and 800 °C, T_f^{TiN}=750 and 830 °C, and $T_f^{30\text{ nm C}}$=700 and 770 °C were observed for the 5 nm C, 30 nm TiN, and 30 nm C capping layers, respectively. The difference in formation temperature (which can be observed in Fig. 4) can be attributed to a competition between C, O, and N for the interstitial sites.[9] Without a capping layer, some impurities from the annealing atmosphere can enter the Mo lattice and occupy interstitial sites. These interstitial locations facilitate C diffusion and are therefore important during carbide formation. As a result, the more interstitial sites that are occupied by other elements than C, the harder it is to form the carbide phase, and the higher the formation temperature. We observe that a 5 nm C capping layer already reduces the O diffusion within the Mo film, which makes it easier for the C to occupy the interstitial sites, and we get a lower formation temperature. Increasing the thickness of the C capping layer to 30 nm blocks the O diffusion even more and thus the

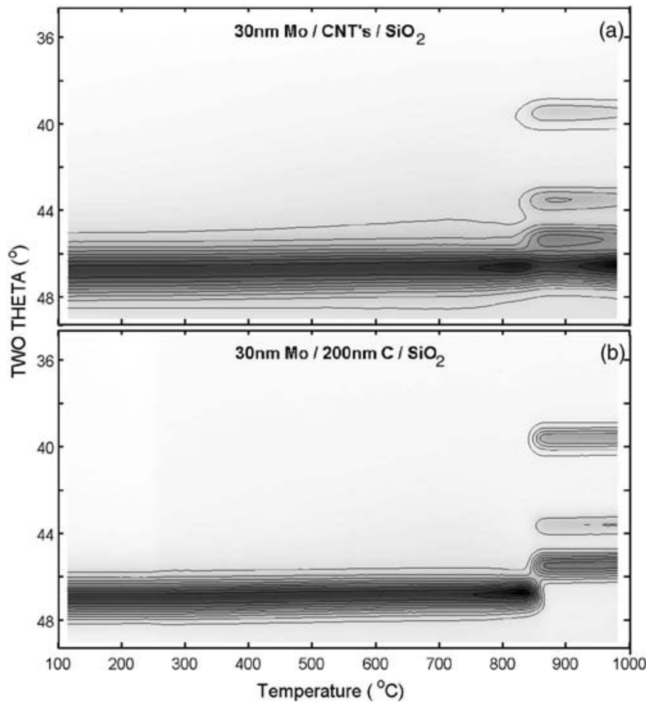

FIG. 5. 30 nm of Mo deposited on (a) CNTs on SiO_2 and (b) 200 nm C on SiO_2 (without a capping layer). The samples were annealed to 1000 °C at 3 °C/s.

formation temperature for the carbide is lowered again. When a 30 nm TiN capping layer is used, there may be some N moving into the Mo lattice, which would explain the increase in formation temperature, compared with the C capping layers.

We measured the resistivity for the Mo_2C phase, $\rho = 59\ \mu\Omega$ cm, and calculated the thickness from crystallographic data,[12] $t = 35.8$ nm, which agrees with the thickness determined by RBS ($t = 38.4 \pm 1$ nm). We also performed *in situ* XRD measurements at heating rates of 0.3, 1, 3, 5, 9, and 35 °C/s. Using the Kissinger formula[13]

$$\ln\left(\frac{dT/dt}{T_f^2}\right) = -\frac{E_a}{k_b T_f} + C, \quad (1)$$

where dT/dt is the heating rate, T_f is the formation temperature, and k_b the Boltzmann constant, a value of $E_a = 3.15 \pm 0.15$ eV was found for the activation energy for Mo_2C formation. Activation energies for C diffusion in carbides are relatively high compared with those in other systems [e.g., 4.5 eV for C in TiC (Ref. 14) versus 2.5 eV for Si in $TiSi_2$, which is the largest value reported in Ref. 15]. Also, from literature[16,17] one knows that the activation energy is usually much higher for C diffusion in a carbide layer than in the metal matrix (e.g., 1.89 eV for C diffusion in Mo). Values reported for C diffusion in Mo_2C range from 3.06 eV (Ref. 18) to 3.60 eV (Ref. 17) in different temperature ranges. Warnes and Simkovich[19] reported a much higher activation energy of 4.79 eV in a temperature range between 800 and 1000 °C. The value for the activation energy, obtained in this work, is in the same range as reported in Refs. 17 and 18.

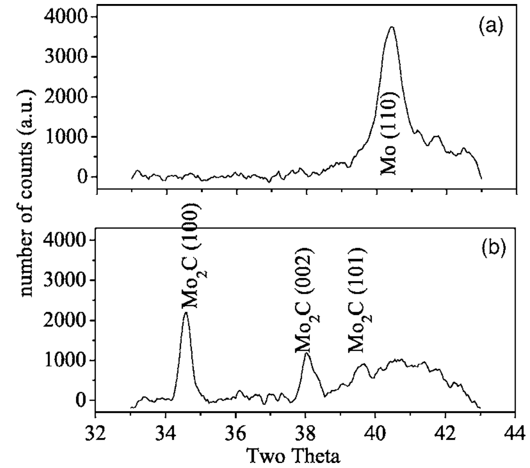

FIG. 6. Standard $\theta/2\theta$ (Cu $K\alpha$) of 30 nm Mo deposited on CVD diamond: (a) unreacted Mo, and (b) annealing to 1000 °C (without a capping layer) results in Mo_2C formation.

C. Reaction with CNTs and diamond

In this work, amorphous C (*a*-C) was used as a model system to investigate the carbide formation. To verify if the results obtained for reaction of a metal with *a*-C directly relate to the reaction with diamond or CNTs, the reaction of Mo was also tested on these C substrates. Therefore, a layer of CNTs was dispersed on the SiO_2 substrate and covered with 30 nm of Mo. In Fig. 5 the *in situ* XRD pattern of the reaction of Mo and CNTs can be compared with the reaction of Mo and *a*-C, which was discussed above. With the Mo–CNT system, a part of the Mo reacts with these CNTs to form the stable Mo_2C, while the remaining Mo stays unreacted on the substrate. Notice that the Mo_2C phase is formed at about the same temperature as for the *a*-C sample and the CNT sample, showing that $T_f^{Mo_2C}$ is independent of the chemical nature of the substrate. The same experiment was done with Ti and CNTs, but the Ti tends to react with the SiO_2 substrate and/or with the oxygen impurities left in the annealing chamber, instead of reacting solely with the CNTs. This may cause problems when using Ti in advanced devices with CNTs. As further evidence, 30 nm Mo was deposited on chemical vapor deposited (CVD) diamond and annealed to 1000 °C at the standard heating rate of 3 °C/s. Figure 6 shows standard $\theta/2\theta$ XRD patterns measured *ex situ* (using Cu $K\alpha$ radiation). There is a clear difference between the as-deposited sample (a) and the annealed sample (b). This evidences that the carbide formation for the Mo–C system is independent of the chemical nature of the carbon-to-carbon bonding in the substrate.

In this work, we have mainly focused on the formation of carbides. Of course, for practical applications as a contacting material to carbon-containing semiconductors, the electrical nature of the carbide-semiconductor interface will also be important. Unfortunately, the use of amorphous carbon substrates during most of our experiments did not allow for an investigation of contact resistance. Undoubtedly, the contact resistance will vary depending on the semiconductor that is used (e.g., SiC versus diamond). For contacts to diamond, Nakanishi *et al.*[20] reported electrical measurements for Mo

contacts to boron-doped polycrystalline diamond films. For diamond with a resistivity of 13 Ω cm, they found a contact resistance of $\sim 10^{-2}$ Ω cm^2 for as-deposited Mo. Annealing of this sample for 60 min at 600 °C resulted in the formation of Mo_2C and in an improved contact resistance of $\sim 10^{-3}$ Ω cm^2. As-deposited Ti contacts on these diamond substrates exhibited a contact resistance of $\sim 10^{-1}$ Ω cm^2. Annealing of the Ti at 400 °C for 4 min resulted in an improvement of the contact resistance to $\sim 10^{-3}$ Ω cm^2. For diamond with a resistivity of 0.08 Ω cm, both annealed Ti and Mo films resulted in a contact resistance of $\sim 10^{-6}$ Ω cm^2.

IV. CONCLUSION

In conclusion, we report the formation of molybdenum carbide (Mo_2C) and titanium carbide (TiC) through a solid-state reaction. Mo_2C is a promising alternative to TiC, because its formation is less sensitive to the presence of oxygen. Secondly, the compound Mo_2C only exists over a narrow range of composition (unlike TiC), which will reflect itself in more well-defined physical properties. Also, we have shown for the Mo–C system that the formation temperature is independent of the chemical nature of the carbon-to-carbon bonding in the substrate, and that Mo can be used to form a stable carbide phase with carbon nanotubes and diamond.

ACKNOWLEDGMENTS

The authors would like to thank R. A. Carruthers for thin film deposition, R. Martel and J. Chen for the nanotube samples, A. Hikavyy for the CVD diamond substrate, and J. Jordan-Sweet for help with the XRD beam line. The synchrotron XRD experiments were conducted under DOE Contract No. DE-AC02-76CH-00016. One of the authors (C. D.) acknowledges the Nationaal Fonds voor Wetenschappelijk Onderzoek-Vlaanderen for financial support.

[1] J. A. Cooper and A. Agarwal, Proc. IEEE **90**, 956 (2002).
[2] V. K. Bazhenov, I. M. Vikulin, and A. G. Gontar, Sov. Phys. Semicond. **19**, 829 (1985).
[3] P. Avouris, Chem. Phys. **281**, 429 (2002).
[4] S. L. Zhang and M. Ostling, Crit. Rev. Solid State Mater. Sci. **28**, 1 (2003).
[5] T. Tachibana, B. E. Williams, and J. T. Glass, Phys. Rev. B **45**, 11975 (1992).
[6] K. L. Moazed, J. R. Zeidler, and M. J. Taylor, J. Appl. Phys. **68**, 2246 (1990).
[7] R. Martel, V. Derycke, C. Lavoie, J. Appenzeller, K. K. Chan, J. Tersoff, and P. Avouris, Phys. Rev. Lett. **87**, 256805 (2001).
[8] T. B. Massalski, Metall. Trans. B **20**, 445 (1989).
[9] H. J. Goldschmidt, *Interstitial Alloys* (Butterworths, London, 1967).
[10] W. S. Williams, JOM **49**, 38 (1997).
[11] W. S. Williams, Phys. Rev. **135**, A505 (1964).
[12] J. R. Chen, J. Vac. Sci. Technol. A **5**, 1802 (1987).
[13] E. G. Colgan and F. M. d'Heurle, J. Appl. Phys. **79**, 4087 (1996).
[14] S. Sarian, J. Appl. Phys. **39**, 3305 (1968).
[15] P. Gas and F. d'Heurle, in *Properties of Metal Silicides*, edited by K. Maex and M. Van Rossum (INSPEC, London, 1995), p. 279.
[16] Y. Hiraoka, H. Iwasawa, T. Inoue, M. Nagae, and J. Takada, J. Alloys Compd. **377**, 127 (2004).
[17] G. Samsonov and A. Epik, Dopov. Akad. Nauk Ukr. RSR **1**, 67 (1964).
[18] C. J. Rosa, Metall. Trans. A **14**, 199 (1983).
[19] B. M. Warnes and G. Simkovich, J. Less-Common Met. **106**, 241 (1985).
[20] J. Nakanishi, A. Otsuki, T. Oku, and O. Ishiwata, J. Appl. Phys. **76**, 2293 (1994).

Journal of Applied Physics is copyrighted by the American Institute of Physics (AIP). Redistribution of journal material is subject to the AIP online journal license and/or AIP copyright. For more information, see http://ojps.aip.org/japo/japcr/jsp